Journal of Biomedical Optics 11(1), 014033 (January/February 2006)

Dialysis-assisted fiber optic spectroscopy for *in situ* biomedical sensing

P. Blazkiewicz
K. Blazkiewicz
A. Verhaege
The University of Queensland
School of Physical Sciences
Centre for Biophotonics and Laser Science
St. Lucia QLD 4072 Australia
E-mail: blazkie@physics.uq.edu.au

Y. G. Anissimov
M. S. Roberts
The University of Queensland
Princess Alexandra Hospital
Therapeutic Research Unit
St. Lucia QLD 4072 Australia

A. V. Zvyagin
The University of Queensland
School of Physical Sciences
Centre for Biophotonics and Laser Science
and School of Information Technology and
Electrical Engineering
St. Lucia QLD 4072 Australia

Abstract. A miniature fiber optic spectrometer enclosed within a semipermeable (dialysis) membrane is proposed for *in vivo* interstitial sensing applications. The semipermeable membrane acts as a molecular filter, allowing only small molecules to pass through to the sampling volume. This filtering, in principle, should enable continuous *in vivo* drug sensing, removing the necessity for complex microdialysis systems. We use a biological phantom to examine the reliable detection of a fluorescence signal from small dye molecules in the presence of large fluorophores and scatterers. We find that spectral artefacts arising from scatterers and large fluorophores are substantially suppressed, simplifying the spectral analysis. In addition, the measured sampling rate of 157 s is superior to existing *in vivo* tissue assaying techniques such as microdialysis, which can take tens of minutes.
 [DOI: 10.1117/1.2166086]

Keywords: fiber optic sensors; fluorescence spectroscopy; microdialysis.

Paper 05188R received Jul. 13, 2005; revised manuscript received Sep. 4, 2005; accepted for publication Sep. 19, 2005; published online Feb. 2, 2006.

1 Introduction

1.1 *In Vivo Fiber Optic Spectroscopy*

Since the 1960s there has been interest in using optical fibers for biomedical sensing.[1] Optical fibers are small and flexible and can be easily inserted into thin catheters or hypodermic needles. They are typically made of glass or plastic, which are nontoxic, chemically inert, and immune to electromagnetic interference and crosstalk.[2] Such properties can, in principle, offer reliable, minimally invasive *in vivo* monitoring without harmful effects to patients.

In sensing applications, optical fibers are typically used to deliver and collect light from a probe, which interacts with a remote sampling region. This probe can simply be a cleaved fiber tip, or it may be a more complex optical component.[3] Light sent to the sample via the probe has a unique signature imprinted onto its spectral profile due to light-tissue interactions. This signature bears information about the tissue content. The major light-tissue interaction modes are absorption and scattering. If fluorophores are present, then light absorption is followed by the production of longer wavelength radiation via fluorescence. Light-tissue interactions via elastic scattering randomize the propagation direction of light after each scattering event. The cumulative effect of these light-tissue interactions can be very complex. This is due to the abundant presence of tissue scattering constituents, such as endogenous fluorophores, pigments, and cells.

A typical method of reducing the complexity of the return signal is to introduce a selective element into the fiber probe tip. For example, during the 1980 to 1990s fiber probes incorporated what is known as an optrode[4–8] ("optical electrode"). In the optrode approach, the optical fiber guides light to and from a special chemical reagent. The reagent's absorption, fluorescence, or lifetime is affected by the concentration of a specific target chemical, which is detected in the return signal. This gives the fiber probe a very selective response related to a single chemical species. The reagent must be immobilized and kept at the tip of the fiber probe. One method is to impregnate the reagent into a polymer or membrane and attach it to the tip of the fiber.[4,8] In the second method, the reagent is trapped inside a sampling volume at the tip of the fiber probe using a membrane.[5,6] The selected membrane is permeable to the chemical of interest, but it prevents escape of the reagent.

An issue with optrode chemical sensors is that they rely on chemical reactions to modulate the detected optical sensor signal. The chemical reagent stability is typically limited, thus shortening the useful working life of optrode fiber sensor. The response time of optrode sensors can be rapid in the case of impregnated membranes. However, optrodes are very selective and produce a response for only a specific chemical. If multichemical detection is required, then multiple reagents and wavelength multiplexing systems are required.[4] This increases system complexity, decreases reliability, and limits the possible applications of the designed fiber probe.

Many of these optrode systems have been used to measure pH, O_2, and CO_2 concentrations in arteries and veins.[4,5,7,8]

Address all correspondence to Paul Blazkiewicz, Centre for Biophotonics and Laser Science, School of Physical Sciences, University of Queensland, Sir Fred Schonell Drive, Brisbane, Queensland 4072, Australia, Tel: +61733653411. Fax: +61733651242. E-mail: blazkie@physics.uq.edu.au

1083-3668/2006/11(1)/014033/7/$22.00 © 2006 SPIE

These systems were attractive as there is no risk of harmful physiological effects due to mobile dye molecules.[6] However, in commercially available systems, consistency and reliability were unacceptable.[9] This was due to significant malfunctions and inconsistencies that were attributable to the intra-arterial environment.[9]

Another method of processing *in vivo* spectroscopic information is to use sophisticated numerical methods, such as photon diffusion models. Several "success stories" of fiber optic spectroscopy include noninvasive measurement of bilirubin in neonates,[10] and *in vivo* monitoring of blood oxygenation.[11] For these models to work, a number of parameters characterizing living tissue must be known accurately. As such, this approach is susceptible to minute variations in tissue condition and is generally prone to measurement artifacts. One can see that both the optrode and photon diffusion techniques are less than adequate, if a general type of fiber probe is required.

1.2 *Drug Monitoring and Microdialysis*

It is known that a common site of drug action in the body is within its tissues. The ability to better monitor and understand drug distribution inside various tissues can lead to improved dosing strategies for a number of patient groups.[12,13] The development of new research tools for analyzing *in vivo* drug concentrations in body tissues represents an important research goal. Methods that enable continuous monitoring of drug levels can give information about drug penetration, transport, distribution, and pharmacokinetics inside body tissues. Continuous *in vivo* drug monitoring is especially useful when drugs with a narrow therapeutic index are used, or where imprecise dosing can lead to substandard outcomes for patients.

Currently, typically only the blood concentration of drugs has been readily available in most human studies. There are limited instrumental options available for measuring drug concentration in other tissues, such as muscle, fat, and dermis. The use of biopsies to obtain tissue concentrations is not only painful, invasive, and time consuming but usually provides information only at a single discrete point in time.

In the 1980s a new minimally invasive technique for continuous drug *in vivo* monitoring was developed called microdialysis.[14–17] In microdialysis a semipermeable dialysis membrane tube is inserted into tissue and perfused with a buffer solution. Drug molecules from the intercellular tissue region diffuse across the membrane into the buffer solution. This buffer solution and drug molecules are pumped out of the tube, collected, and analyzed. The microdialysis technique has been widely used, but there are several fundamental problems. Drug concentration in the buffer solution does not generally reflect drug concentration in the tissue.[18] Second, the establishment of dynamic equilibrium is a lengthy process, due to continuous renewal of the buffer solution in the head, which flows into a fraction collector. The sampling rate is slow, with the first reading being tens of minutes after probe insertion. The permeated drugs are thinly spread between the catheters and fraction collector, compromising the readout rate, and/or the sensitivity of the microdialysis technique. Also, the necessary use of a catheter and a fraction collector makes further miniaturization of microdialysis devices problematic. The outlined problems of microdialysis could be solved if measurements were taken locally, inside the sampling head.

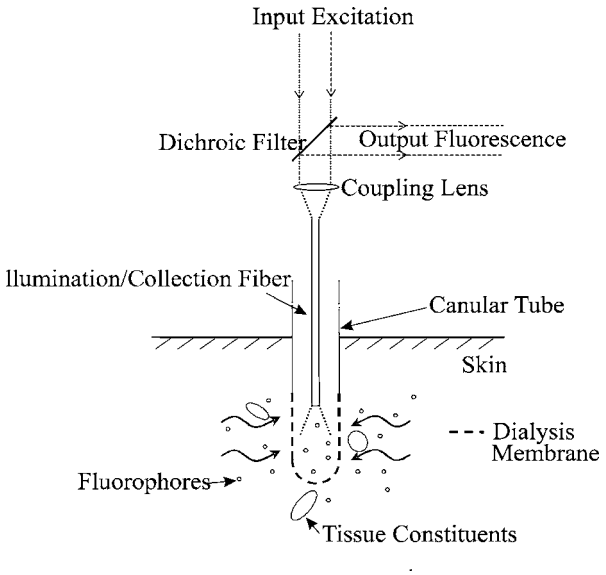

Fig. 1 Schematic diagram of DAFOS using a single fiber for illumination and collection.

2 Dialysis-Assisted Fiber Optic Spectroscopy

The combination of a fiber optic sensor and a semipermeable membrane has been addressed for specific biomedical applications.[4–8,19,20] However, the reported approaches rather underscore the true potential it might confer, that is, detection of exogenous molecules, such as drugs, and also, small molecules of endogenous origin inside body tissue.

We propose to combine fiber optic spectroscopy and microdialysis into a technique called dialysis-assisted fiber optic spectroscopy (DAFOS). The key feature of the DAFOS system is the sampling head probe, which has a fiber optic probe enclosed in a hydrophilic dialysis membrane (see Fig. 1). The membrane surrounding the sampling head enables molecules of small molecular weight to diffuse through the membrane while blocking larger sized molecules. However, unlike in microdialysis, we now optically monitor the contents of the sampling volume locally via a fiber optic probe. The ultimate goal of DAFOS is to monitor drug concentrations locally in tissue. For such applications it is fortunate that most drugs have a small molecular weight, and low affinity to proteins, enabling their permeation into the sample head. This should enable sufficient isolation between the target chemicals/drugs and the constituents of the surrounding tissue.

Unlike microdialysis, DAFOS is a stationary and miniature system, which renders it rapid, sensitive, and a reliable spectroscopic chemical analyzer. A rapid response is achieved due to the small volume of the sampling head. This enables equilibrium with the surrounding environment within minutes, not in tens of minutes as in microdialysis. Since equilibrium is established through passive diffusion, the DAFOS dynamics are simpler and more tractable compared to microdialysis.

The system tested in this paper measures fluorescence with one multimode optical fiber (see Fig. 1). Laser light is deliv-

ered to the sampling volume through the optical fiber, enabling the excitation of fluorophores. After absorption, these excited fluorophores then reemit light at a longer wavelength (fluorescence). This fluorescence is collected by the same optical fiber and guided in the opposite direction to the excitation light. The return signal is then passed through a dichroic filter to remove any scattered laser light. This filtered return signal is then directed to a spectrometer for analysis.

In this paper, the feasibility of using the membrane as an *in situ* molecular filter for fiber optic spectroscopy is tested. We perform modeling and experiments on the fiber probe collection efficiency to determine the minimum required sampling volume size. Finally, modeling and experimental tests are performed to see if the response time constant is competitive with the standard microdialysis.

3 DAFOS Design Considerations

To design a suitable DAFOS probe, we must know how localized the fluorescence collection efficiency is near the fiber probe tip. This will indicate the minimum DAFOS probe size that can be used. Second, the response time of the probe must be shorter than that achieved with microdialysis. The response time is limited by perfusion through the membrane and diffusion inside the sampling volume. The perfusion time through the membrane is material dependent, but the diffusion time depends on the buffer solution and the probe geometry. In this section, we calculate the expected collection efficiency and response time of a simple DAFOS system.

3.1 *Fiber Collection Efficiency and DAFOS Probe Size*

The optical field emerging from the distal end of a multimode fiber can be modeled as a Gaussian beam. For a first-order approximation, it is sufficient to assume that in the near field, the beam has constant radius equal to the fiber core radius (r_c). This beam has a uniform irradiance across its lateral cross section. In the far field, the output beam is modeled as a cone of light, with uniform irradiance across its lateral cross section. The cone angle is equal to the acceptance angle of the optical fiber, given by $\theta_a = \arcsin(\mathrm{NA}_f/n_m)$, where NA_f is the fiber numerical aperture, and n_m is the refractive index of the surrounding medium. Under these simplifying assumptions, the output irradiance of the fiber is reduced to

$$I_{\mathrm{in}} = \begin{cases} P_{\mathrm{in}}/(\pi r_c^2) & \text{near field} \\ P_{\mathrm{in}}/(4\pi z^2 \mathrm{NA}_f^2) & \text{far field,} \end{cases} \tag{1}$$

where P_{in} is the power of the excitation light and z is the distance from the end of the fiber tip. Knowing the irradiance profile of the excitation beam, we can calculate the fluorescence power generated in a specified sampling volume by the following equation:

$$P_{\mathrm{fluo}} = \int_{V_{\mathrm{sample}}} \eta \sigma_a n I_{\mathrm{in}} \mathrm{d}V, \tag{2}$$

where η is the quantum efficiency of the fluorophore, σ_a is its absorption cross section (cm^2), and η is the fluorophore concentration (in cm^{-3}). The integration of Eq. (2) is simplified into a 1-D integration over the z axis using the conditions of Eq. (1). Taking into account Eq. (1) and the cylindrical symmetry of the configuration, the collected fluorescence power P_{cf} is given by

$$P_{\mathrm{cf}}(z_0) = \int_0^{z_0} \int_0^{\infty} \frac{\mathrm{d}P_{\mathrm{fluo}}}{\mathrm{d}z} \frac{\Delta\Omega(\rho,z)}{2} \mathrm{d}\rho\, \mathrm{d}z$$

$$= P_{\mathrm{in}} \sigma_a n \int_0^{z_0} \int_0^{\infty} \frac{\Delta\Omega(\rho,z)}{2} \mathrm{d}\rho\, \mathrm{d}z, \tag{3}$$

where $\Delta\Omega(\rho,z)$ is the solid angle of fluorescence light that reaches the fiber core within its acceptance cone, ρ is the radial position away from the fiber axis, z is the axial distance from fiber tip, and z_0 is the maximum axial distance at which the fluorescence is collected.

The functional representation of $\Delta\Omega(\rho,z)$ depends on the position of the fluorophore with respect to the optical fiber tip. We have considered three main cases, as illustrated in Fig. 2. In case 1, fluorophores are located within one Rayleigh range from the fiber tip (near field), and within one core radius (r_c) from the fiber axis. In case 2, fluorophores are beyond one Rayleigh range from the fiber tip (far field), but still within one core radius from the optical axis, i.e., $\rho \leq r_c$. In case 3, the fluorophores are again located in the far field, but are located more than the core radius away from the optical axis, i.e., $\rho > r_c$. We find the fluorescence collection efficiency by performing the integration shown in Eq. (3) to obtain the collected fluorescence power $P_{\mathrm{cf}}(z_0)$, and then dividing it by the input excitation power (P_{in}).

The dependence of fiber collection efficiency versus the sampling volume depth (z_0) is shown in Fig. 3. From Fig. 3, it is clear that under our experimental conditions fluorophores in the close vicinity of the fiber (1–2 mm) primarily contribute to the return signal. This indicates that a membrane enclosed sampling volume of several millimeters in length is sufficient

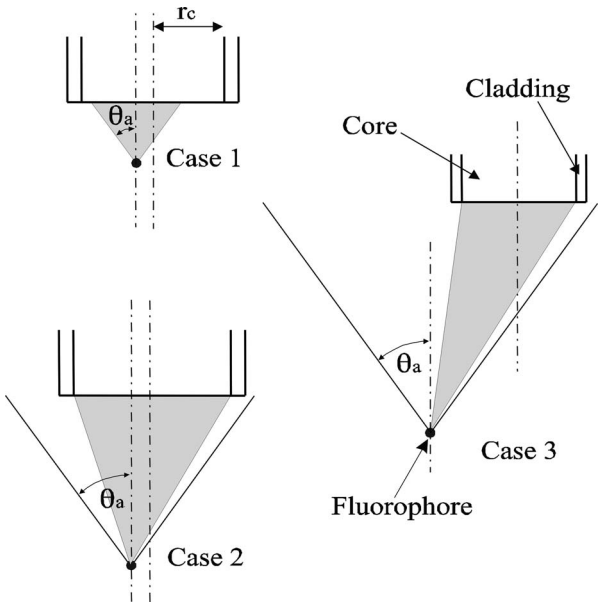

Fig. 2 Three fluorescence collection geometries used in the theoretical modeling; shaded regions indicate cone of collected fluorescence light (see text for details).

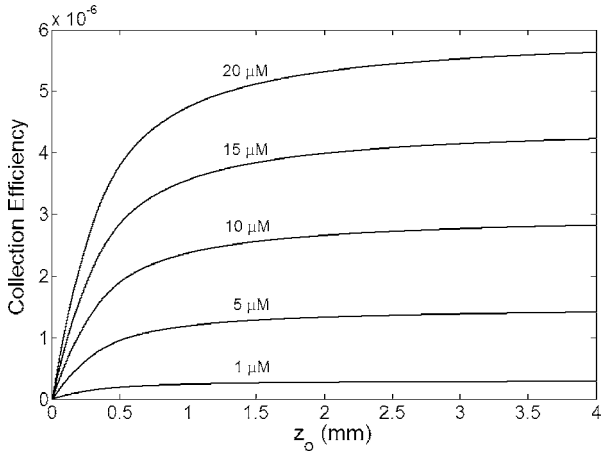

Fig. 3 Theoretical fluorescence collection efficiency curves for a single fiber probe immersed in rhodamine:6G (Rh:6G), using molar concentrations in the range 1 to 20 μM. The NA and core diameter of the fiber were 0.22 and 105 μm, respectively; the refractive index of the sampling volume was 1.34; and the quantum efficiency (η) was set to unity.

to collect the fluorescence signal. Cooney et al. have reported similar theoretical modeling with this fiber probe geometry in the context of Raman spectroscopy.[21]

3.2 *Response Time Constant of DAFOS*

Unlike traditional microdialysis, the main operation mode of DAFOS is stationary, there is no convective buffer flow in the sampling head. DAFOS is governed by the following two processes: permeation of fluorophores through the membrane and diffusion of fluorophores outside and inside of the sampling head. To estimate the expected response time, we model the DAFOS probe as a long tube of radius r_0, characterized by the permeation constant P (in centimeters per second). The fluorophore concentration inside the probe is $c(t)$, versus time t, and the initial concentration of fluorescent drug molecules outside the tube is c_m. Equilibrium between inner and outer regions is established by permeation and diffusion. In the standard diffusion theory framework, the equilibrium process can be approximated by the following relationship:

$$c(t) = \frac{1}{t_{\mathrm{eq}}} \int_0^t \exp[-(t-\tau)/t_{\mathrm{eq}}] c_m(\tau)\, \mathrm{d}\tau, \qquad (4)$$

where t_{eq} is the equilibrium time. The equilibrium time (t_{eq}) is the sum of the diffusion and permeation times: $t_{\mathrm{eq}}=t_{\mathrm{diff}}+t_{\mathrm{perm}}$, where $t_{\mathrm{diff}}=r_0^2/(5.76D)$ is the diffusion time, D is the diffusion constant (cm^2/s), and $t_{\mathrm{perm}}=2r_0/P$ is the permeation time. Assuming that $t_{\mathrm{diff}} \gg t_{\mathrm{perm}}$, and using typical parameters of our DAFOS system, $r_0=0.05$ cm, $D=2.8\times10^{-6}\ \mathrm{cm}^2/\mathrm{s}$ for Rh:6G in water[22] and $D=3.6\times10^{-6}\ \mathrm{cm}^2/\mathrm{s}$ for Rh:B in water,[23] the t_{diff} equilibration time is calculated to be 155 and 121 s, respectively. Such a short response time constant represents a very attractive target for biomedical drug sensing applications. It is also smaller than the time constants achievable with standard microdialysis, indicating that DAFOS may be a feasible drug analysis technique.

4 Experiment

To carry out a preliminary experimental study of DAFOS, a laboratory system prototype was built. It consisted of three main parts: a fiber-optic spectrometer, a sampling head, and liquid biological phantoms. The miniature fiber optic spectrometer was configured as shown in Fig. 1. The outer cladding diameter, core diameter, and numerical aperture (NA_f) of this fiber were 125 μm, 105 μm, and 0.22, respectively. A 1.2-mW laser of wavelength of 532 nm was used as the illumination source. This illumination source was coupled into the multimode fiber (coupling efficiency of 69%) and delivered to the sampling head. A dichroic filter (wavelength cutoff, 540 nm) was used to separate the illumination radiation from the fluorescence radiation collected by the distal end of the fiber. The collected fluorescence radiation was coupled into a computer-controlled scanning single-grating Czerny-Turner spectrometer (Acton Research Corporation, SpectraPro® 275, $f/3.8$, wavelength resolution 1.6 nm) terminated by a *p-i-n* photoreceiver.

The sampling head comprised a sealed membrane tube filled with water, in which the fiber distal end was immersed. The filtering performance of the membrane is determined by its molecular cutoff. Molecular cutoff is defined as the molecular weight measured in daltons, at which 80% of the molecules are prevented from passing through the membrane. The selected dialysis membrane had a molecular cutoff of 20,000 Dal, which was sufficient to pass fluorophores of interest (fluorescent dyes, molecular weight $<$500 Dal), but prevent passing micrometer-sized particles, which cause significant scattering.

In the biological phantom, rhodamine:6G dye (Rh:6G) was used to represent a drug (exogenous fluorophore). The endogenous tissue fluorophores were mimicked by micrometer-sized dye-doped beads (PC-Red™, Fluoresbrite® polychromatic red microspheres, diameter 2.0 μm, 5.68×10^9 particles/ml, $\lambda_{\mathrm{emission}}=584$ nm), which were unable to penetrate through the membrane. The scattering tissue was mimicked by an aqueous suspension of nonfluorescent 2- and 5-μm polystyrene spheres (15% by weight). In our experiments, 1 μM of Rh:6G was dissolved in a water/methanol solution of equal volume ratio. This 1-μM concentration was tested, as it is a typical *in vivo* drug concentration that can be achieved via the common drug delivery pathways. The liquid biological phantom was placed in a vial, and then the sampling head was immersed into the solution. The fluorescence signal was acquired by the spectrometer and the collected data was transferred to a PC for display, analysis, and archiving. The acquired spectra were processed to correct for the dichroic filter wavelength response, and also, to remove the instrumental high-frequency noise by lowpass filtering. The acquired fluorescence signals using different biological phantoms were then normalized for comparison.

5 Results

5.1 *Effect of the Dialysis Membrane on Spectroscopic Artefact Suppression*

The spectral shape of the Rh:6G fluorescence signal was acquired in a clear solution [Fig. 4(a), solid line] to serve as a reference signal. Then the fluorescence response was tested in

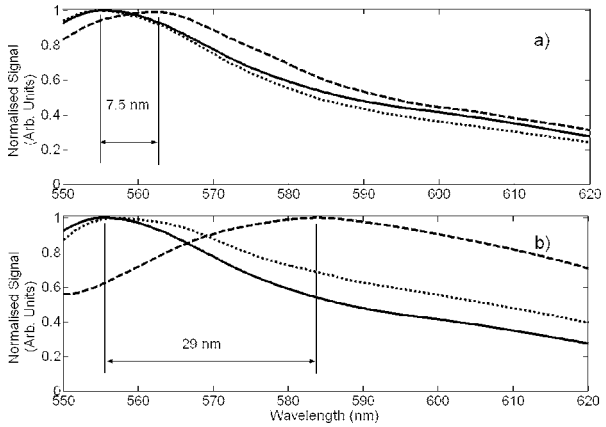

Fig. 4 (a) Plot of Rh:6G fluorescence spectrum using bare fiber probe in clear solution (solid line), bare fiber probe in scattering phantom (dashed line), and DAFOS probe in scattering phantom (dotted line) and (b) plot of Rh:6G fluorescence spectrum using bare fiber probe in clear solution (solid line), bare fiber probe in fluorescent phantom (dashed line), and DAFOS probe in fluorescent phantom (dotted line).

the presence of nonfluorescent scatterers (dashed line) and without a membrane enclosure, shown in Fig. 4(a). It was found that the fluorescence peak appeared to be red-shifted by 7.5 nm in the presence of nonfluorescent scatterers. Next the test was repeated using our membrane-enclosed DAFOS probe, which resulted in efficient suppression of the spectroscopic artefacts due to the scatterers [Fig. 4(a), dotted line]. Typically, the scatterer-affected peak was observed to occur either red-shifted in wavelength, as in Fig. 4(a), or blue-shifted, depending on the scatterer size and concentration. We speculate that it might result from the intricate interplay of several scattering properties of nonabsorbing scatterers versus wavelength: scattering cross section, scattering anisotropy factor g, and probability of multiple scattering.

Next the DAFOS response to the presence of endogenous fluorophores was tested. This was realized by using the liquid biological phantom containing fluorescent polystyrene spheres PC-red. The fluorescence peaks of the exogenous and endogenous fluorophore phantoms were separated in wavelength by 30 nm, so that the obscuring effect was profound. Indeed, the spectroscopic signature of the exogenous fluorophores phantom [Fig. 4(b), solid line] was completely distorted in the presence of the high-concentration endogenous fluorophore phantom (PC-red), as shown in Fig. 4(b) (dashed line). The enclosure of the sampling head with a dialysis membrane enabled considerable suppression of these spectroscopic artefacts, see Fig. 4(b) (dotted line). This was due to the filtering property of the dialysis membrane that prevented micrometer-sized PC-red particles from entering the sampling head. The residual red-shift of the filtered spectroscopic signal in DAFOS is believed to be due to the fluorescent contribution of the endogenous fluorophore phantom (PC-red) situated outside the sampling head.

5.2 *Detection Depth Range and Sensitivity*

To demonstrate the localized nature of the fluorescence signal, the collected fluorescence power was measured versus the axial distance from the fiber tip. The fluorescence spectrum was measured using the spectrometer over the range of 530 to 650 nm, with an integration time of 250 ms per point. Numerical integration over the recorded spectrum was performed to obtain the total collected fluorescence power. The membrane was not required for this measurement, which was carried out in a clear Rh:6G solution. The axial signal variation was measured by adjusting the separation between the fiber tip and the base of a black container filled with the Rh:6G solution. The measurement commenced by bringing the fiber tip into contact with the base of the container, which corresponded to the signal with no fluorophores. The successive measurements of signal power were taken by raising the fiber probe above the container base, enabling a larger volume of fluorophores to be sampled. The result of these measurements is plotted in Fig. 5(a), marked by asterisks.

The solid line in Fig. 5(a) is a theoretical fit to the experimental data points using Eq. (3). This graph confirms that the major contribution to the DAFOS fluorescence signal comes from the volume within 1.4 mm from the tip of the optical fiber, measured at the 90% signal fall off.

To determine the detection sensitivity of the fluorescence DAFOS system, the detected fluorescence power was plotted versus Rh:6G molar concentration, over the range of 10 to 100 μM, as shown in Fig. 5(b). As expected, this dependence was linear, with a slope of 0.431 pW/μM. Intersection of this signal line with the fluorescence signal detection threshold (noise floor) yielded a minimum detectable concentration of 340 nM.

5.3 *Response Time*

Since the operation rate represents an important performance indicator of the proposed technique, we carried out measurements of the equilibrium time. The peak detected fluorescence signal in a 1-mM aqueous solution of rhodamine B (Rh:B) was measured versus time using the DAFOS system, and the result is plotted in Fig. 6. The data points were normalized to the signal saturation value.

A theoretical curve (solid line) was fit to the data using Eq. (5). The estimated time constant of this exponential theoretical curve yields an equilibrium time $t_{eq}=157$ s. This measured time constant was found to be 36 s longer than the theoretical value of 121 s, assuming a negligible permeation time constant. Thus, the permeation time constant was not negligible, but approximately 30% of the expected diffusion time constant. To increase the DAFOS operation rate the radius of the dialysis membrane tube can be reduced. This will decrease both the permeation and radial diffusion time constants. Despite a permeation time constant of the order of 2 min, the demonstrated equilibrium time is already superior compared to the existing tissue assaying techniques, including microdialysis.[14]

6 Discussion

We demonstrated that the DAFOS technique is capable of detecting small-molecular-weight fluorescent molecules of interest in the presence of an obscuring spectral environment. The clear suppression of contributions from endogenous fluorophore and scattering agents was demonstrated. The filtering efficiency of the DAFOS laboratory system prototype, however, has room for improvement. In the case of the endog-

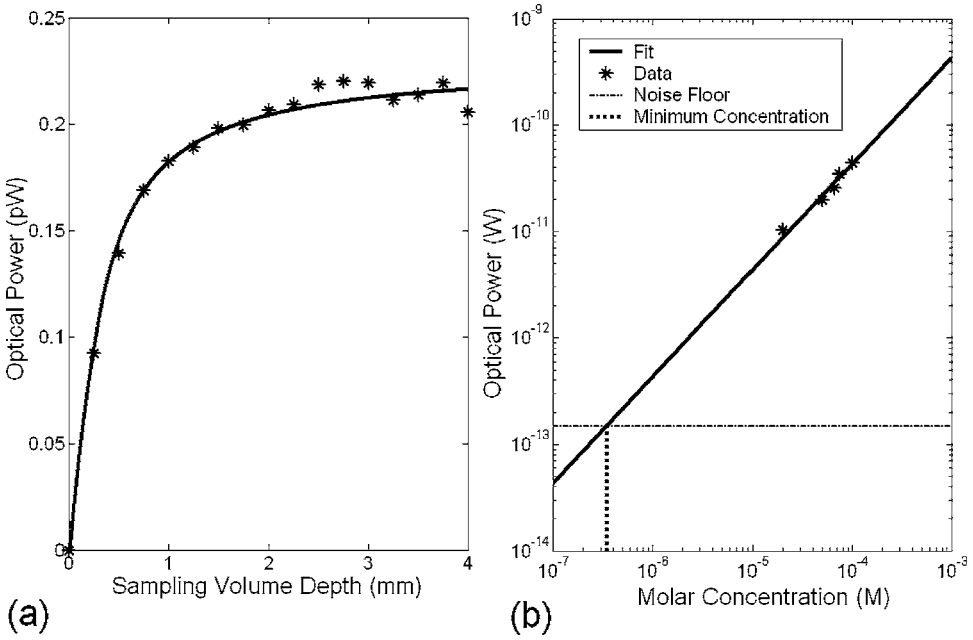

Fig. 5 (a) Fluorescence signal power versus sampling volume depth: experiment (*), theoretical fit (solid line). Concentration of Rh:6G is 1 μM. (b) Plot of the fluorescence signal power versus the fluorophore (Rh:6G) concentration: experiment (*), linear fitting (solid line), noise floor (dashed-dotted line).

enous fluorophore phantom (PC-red), the filtered fluorescence spectrum of the liquid biological phantom (Rh:6G) remained slightly distorted. We observed optical leakage of the 532-nm excitation light through the membrane during experiments. It is possible that the spectral distortion is due to unwanted excitation of the fluorophores outside the sampling head. This external excitation results in a nonnegligible contribution to the detected fluorescence signal. To alleviate this problem, an optically opaque membrane could be used to confine the excitation radiation inside the sampling head. The use of an optically opaque dialysis membrane would also permit the use of intense ultraviolet (UV) radiation *in vivo*, which otherwise represents a mutagenic hazard.[24] For a broad range of molecular species, rich and detailed spectral information is available in the UV spectral range. It is believed that a safe technique for performing UV spectroscopy *in vivo* would enable a thorough and comprehensive analysis of drug concentration in tissue.

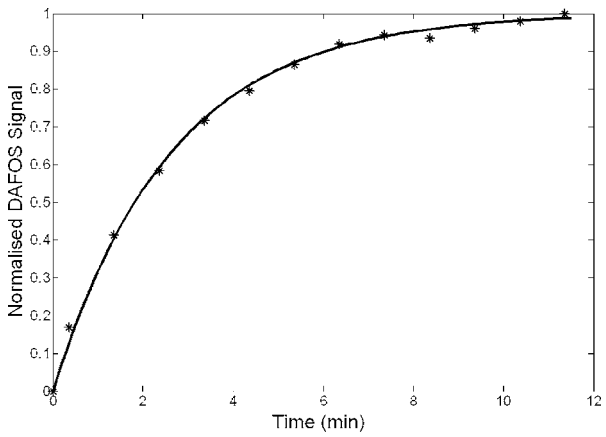

Fig. 6 Plot of the normalized DAFOS signal versus time: experiment (*), theoretical fitting curve (solid line).

We envisage several possible approaches to improve the DAFOS system sensitivity to fluorophore concentration. An increase of the excitation power in combination with an optically opaque membrane in the DAFOS sampling head is the most straightforward approach. It will increase the overall fluorescence yield, in addition to the suppression of unwanted external contributions. Another approach involves the tradeoff between spectrometer resolution and its throughput. By increasing the spectrometer slit width, the optical throughput can be increased significantly. However, this increase in optical throughput reduces the resolution of the spectrometer, which may be detrimental to the spectral analysis of the sampling volume. Typically in fiber optic spectroscopy, fiber bundles are used to improve the fluorescence collection efficiency.[13] However, in our experimental configuration the choice of the sampling head was constrained by the membrane diameter of 0.5 mm, which precluded the use of a large number of collection fibers. A more practical method would be to use a fiber with a larger core diameter and NA_f to improve the collection efficiency. Using a commercially available optical fiber with a core diameter of 0.4 mm and NA_f of 0.37, a factor of 6 increase in collection efficiency is expected.

7 Conclusion

A new technique called DAFOS, suitable for drug sensing *in vivo*, was proposed and demonstrated. The combination of fiber optic spectroscopy and microdialysis enables efficient suppression of the complex background spectrum that has plagued *in vivo* biomedical sensing applications. We carried

out the feasibility study of DAFOS employing a laboratory system prototype and using liquid biological phantoms. Strong suppression of the fluorescence artefacts due to the presence of endogenous fluorophores and scatterers was demonstrated. It was shown theoretically and experimentally that fluorophores are detected locally. The unprecedented operation rate of the DAFOS prototype in comparison with the traditional tissue assaying techniques was demonstrated. As a result of this preliminary study, DAFOS was demonstrated to have strong promise as a research and analytical tool for rapid, reliable sensing of exogenous fluorophores in live tissue. In particular, DAFOS applications for sensing of minute transient traces of drugs in living tissue are envisaged.

Acknowledgments

The authors acknowledge the financial support of the University of Queensland Research Development Grant (2005).

References

1. N. S. Kapany and N. Silbertrust, "Fiber optics spectrophotometer for *in vivo* oximetry," *Nature (London)* **208**, 138–145 (1964).
2. J. Dakin and B. Culshaw, "*Optical Fiber Sensors Volume 4: Applications Analysis and Future Trends*," Chap. 10, p. 129, Artech House, Norwood, MA (1997).
3. U. Utzinger and R. R. Richards-Kortum, "Fiber optic probes for biomedical optical spectroscopy," *J. Biomed. Opt.* **8**, 121–147 (2003).
4. O. S. Wolfbeis, L. J. Wies, M. J. P. Leiner, and W. E. Ziegler, "Fiber-optic fluorsensor for oxygen and carbon dioxide," *Anal. Chem.* **60**, 2028–2030 (1988).
5. J. I. Peterson, R. V. Fitzgerald, and D. K. Buckhold, "Fiber-optic probe for *in vivo* measurement of oxygen partial pressure," *Anal. Chem.* **56**, 62–67 (1984).
6. O. S. Wolfbeis, "Fiber-optic probe for kinetic determination of enzyme activities," *Anal. Chem.* **58**, 2874–2876 (1986).
7. G. Holst, T. Koster, E. Voges, and D. W. Lubbers, "FLOX—an oxygen-flux-measuring system using a phase-modulation method to evaluate the oxygen-dependent fluorescence lifetime," *Sens. Actuators B* **29**, 231–239 (1995).
8. E. Netto, J. I. Peterson, M. McShane, and V. Hampshire, "A fiber-optic broad range pH sensor system for gastric measurements," *Sens. Actuators B* **29**, 157–163 (1995).
9. E. R. Roupie, "Equipment review: continuous assessment of arterial blood gases," *Crit. Care* **1**, 11–14 (1997).
10. S. L. Jacques, "Path integral description of light transport in tissue," *Ann. N.Y. Acad. Sci.* **838**, 1–13 (1998).
11. J. C. Hebden, A. Gibson, T. Austin, R. M. Yusof, N. Everdell, D. T. Delpy, S. R. Arridge, J. H. Meek, and J. S. Wyatt, "Imaging changes in blood volume and oxygenation in the newborn infant brain using three-dimensional optical tomography," *Phys. Med. Biol.* **49**, 1117–1130 (2004).
12. R. Sauermann, G. Delle-Karth, C. Marsik, I. Steiner, M. Zeitlinger, B. X. Mayer-Helm, A. Georgopoulos, M. Muller, and C. Joukhadar, "Pharmacokinetics and pharmacodynamics of cefpirome in subcutaneous adipose tissue of septic patients," *Antimicrob. Agents Chemother.* **49**, 650–655 (2005).
13. J. F. Thompson, G. A. Siebert, Y. G. Anissimov, B. M. Smithers, A. Doubrovsky, C. D. Anderson, and M. S. Roberts, "Microdialysis and response during regional chemotherapy by isolated limb infusion of melphalan for limb malignancies," *Br. J. Cancer* **85**, 157–165 (2001).
14. P. Lönnroth, P. A. Jansson, and U. Smith, "A microdialysis method allowing characterization of intercellular water space in humans," *Am. J. Physiol.* **253**, E228–E231 (1987).
15. L. Ståhle, S. Segersvärd, and U. Ungerstedt, "Drug distribution studies with microdialysis. II. Caffeine and theophylline in blood, brain and other tissues in rats," *Life Sci.* **49**, 1843–1852 (1991).
16. Y. Hurd, J. Kehr, and U. Ungerstedt, "In vivo microdialysis as a technique to monitor drug transport: correlation of extracellular cocain levels and dopamine overflow in the rat brain," *J. Neurochem.* **51**, 1314–1316 (1988).
17. U. Tossman and U. Ungerstedt, "Microdialysis in the study of extracellular levels of amino acids in the rat brain," *Acta Physiol. Scand.* **128**, 9–14 (1986).
18. J. A. Stenken, "Methods and issues in microdialysis calibration," *Anal. Chim. Acta* **379**, 337–358 (1999).
19. T. Werner, I. Klimant, C. Huber, C. Krause, and O. S. Wolfbeis, "Fiber optic ion-microsensors based on luminescence lifetime," *Mikrochim. Acta* **131**, 25–28 (1999).
20. Y. D. Zhao, A. Richman, C. Storey, N. B. Radford, and P. Pantano, "In situ fiber-optic oxygen consumption measurements from a working mouse heart," *Anal. Chem.* **71**, 3887–3893 (1999).
21. T. Cooney, H. T. Skinner, and S. M. Angel, "Comparative study of some fiber-optic remote Raman probe design. Part I: model for liquids and transparent solids," *Appl. Spectrosc.* **50**(7), 836–848 (1996).
22. R. Brock, M. A. Hink, and T. M. Jovin, "Fluorescence correlation microscopy of cells in the presence of autofluorescence," *Biophys. J.* **75**(5), 2547–2557 (1998).
23. S. A. Rani, B. Pitts, and P. S. Stewart, "Rapid diffusion of fluorescent tracers into *Staphylococcus epidermidis* biofilms visualized by time lapse microscopy," *Antimicrob. Agents Chemother.* **49**(2), 728–732 (2005).
24. C. Brookner, A. Agrawal, E. V. Trujillo, and M. M. Follen, "Safety analysis: relative risks of UV fluorescence spectroscopy and colporoscopy are comparable," *Photochem. Photobiol.* **65**, 1020–1025 (1997).